Oral presentation | Turbulent flow

Turbulent flow-I

Tue. Jul 16, 2024 4:30 PM - 6:30 PM Room B

[6-B-02] Effects of Crossflow Instability on the Development Process of a Turbulent Spot

*Kosuke Nakagawa[1], Shotaro Okazaki[1], Takahiro Ishida[2], Takahiro Tsukahara[1] (1. Tokyo University of Science, 2. Japan Aerospace Exploration Agency)

Keywords: crossflow instability, swept flat plate, turbulent spot

Twelfth International Conference on Computational Fluid Dynamics (ICCFD12), Kobe, Japan, July 14-19, 2024

Effects of Crossflow Instability on the Development Process of a Turbulent Spot

K. Nakagawa*, S. Okazaki*, T. Ishida** and T. Tsukahara*
Corresponding author: tsuka@rs.tus.ac.jp * Tokyo Univ. Science, Japan.
** Japan Aerospace Exploration Agency, Japan.

Abstract: The spread of the turbulent region in boundary layers is one of the well-known problems in the field of fluid dynamics because characteristics such as frictional drag, heat, and mass transfer differ significantly between laminar and turbulent flow. In this study, we investigated this phenomenon on a swept flat plate boundary layer, which simulates a flow field on the leading edge of a swept wing as a flat plate. The swept flat plate boundary layer is a flow field dominated by crossflow instability, and the mechanisms of the turbulent transition process and the spread of the turbulent region are still unclear. Therefore, we investigated the development process of a turbulent spot induced by vortex pairs to clarify the mechanisms of spatial spreading with direct numerical simulation. Hairpin vortices, typical vortex structures in wall turbulence, cause the spatial spread of a turbulent spot. In addition, we found the shedding of traveling crossflow vortices and enhancement of turbulent spot spreading owing to the twisted boundary layer. Clarification of turbulent spreading mechanisms in the swept flat plate boundary layer provides new insights not only into the development process of turbulent spots but also into the self-sustaining mechanisms in a flow field dominated by cross-flow instability.

Keywords: Boundary Layer, Crossflow Instability, Direct Numerical Simulation, Turbulent Spot.

1 Introduction

While there exist various types of wing shapes, current high-speed aircrafts adopt swept wings attached to the fuselage with a sweep angle. The flow field on a swept wing generates a three-dimensional boundary layer because of the difference in the directions of the freestream and the pressure gradient. Such a three-dimensional boundary layer undergoes a crossflow instability accompanied by stationary or traveling crossflow vortices [1]. The crossflow instability amplifies fluctuations caused by roughness and freestream turbulence, inducing crossflow vortices downstream. The formation of crossflow vortices and the process of turbulent transition have been well studied. Brynjell-Rahkola et al. [2] reported the dependence of the cylindrical roughness height on the transition process. Ishida et al. [3] investigated the generation of a turbulent region that started just behind high roughness and spread in the spanwise direction, using a wind tunnel test with a swept flat plate boundary layer. The amplification mechanism of the fluctuation caused by the crossflow instability has been found to change the laminar-turbulent transition process at the roughness height.

As an approach to elucidate the turbulent transition process, one may track the growth process of a turbulent spot. The turbulent spot is a lump of localized finite fluctuations that become amplified downstream, transforming into locally turbulent areas that spread spatially. A typical turbulent spot takes the form of Λ-shape in the two-dimensional boundary layer. In the spot-spreading process, hairpin vortices generated by the local disturbances extend in the freestream direction and away from the wall. Simultaneously, the vortex structures near the wall serve as sources for new hairpin vortices [4]. This cycle repeats, leading to the expansion of the turbulent spot in the spanwise direction in the two-dimensional boundary layer. As for the three-dimensional boundary layer, an experimental study utilizing a rotating disk has revealed the generation of a traveling wave in the upstream region of the turbulent spots [5]. This structure corresponds to the traveling waves previously reported by Ishida et al. [3] and is unique to the three-dimensional boundary layer. Understanding the causes of these peculiar phenomena is important for clarifying the development process of turbulent spots.

Several studies often mentioned a similar characteristic between turbulent spots and bypass transitions in boundary layers. In the transition process, low-frequency fluctuations in freestream turbulence can penetrate the boundary layer and induce low-speed streaks. As these streak structures grow downstream, they collapse owing to the secondary instability on the streaks. These disturbed structures spread over the entire region, similar to the development process of turbulent spots [6, 7]. The distortion of the streak structure is called the sinuous mode [8], and this instability mode also occurs in streak structures induced by cylindrical roughness. This distortion induces hairpin vortices, which collapse the streak structures [9, 10, 11]. Therefore, knowledge of the development and spatial spreading mechanisms of turbulent spots is beneficial to investigate the transition process caused by cylindrical roughness and freestream turbulence. These are also still insufficiently known in the crossflow instability-dominated flow fields.

This study using direct numerical simulation aims to elucidate the specificity of the development process of a turbulent spot in the three-dimensional boundary layers, by comparing the results with those in the Blasius boundary layer as a base flow of two-dimensional boundary layer.

2 Numerical Methods

We used the Falkner–Skan–Cooke (FSC) boundary layer [12, 13] as a base flow with direct numerical simulations (DNSs) to investigate the turbulent transition processes triggered by a turbulent spot in a swept-flat-plate boundary layer and the Blasius boundary layer. The governing equations were the incompressible Navier–Stokes equation and the continuity equation. The Reynolds number of FSC boundary layer was defined as $Re = U_0\delta_0^*/\nu = 337.9$, where δ_0^* is the displacement thickness and U_0 is the external chordwise velocity at the inlet. For the Blasius boundary layer, the Reynolds number was defined as $Re = U_0\delta_0^*/\nu = 593.0$. This difference is attributed to the presence of laminar flow in the spanwise velocity of the FSC boundary layer, so we define it as $U_0 = \sqrt{U_0|_{\mathrm{FSC}}^2 + V_0|_{\mathrm{FSC}}^2}$ in the Blasius boundary layer.

The fractional-step method was used to couple the incompressible Navier–Stokes equation and the continuity equation. The time advancement was carried out using the Crank–Nicolson scheme for the wall-normal viscous diffusion term and the Adams–Bashforth scheme for the other terms. For the spatial discretization, the finite difference method was used: the fourth-order central scheme in the wall-parallel directions with uniform grids, and the second-order central method in the wall-normal direction with non-uniform grids. A nonslip condition was used to the wall surface, and a periodic boundary condition was used in the spanwise direction.

In the upstream region, we used the initial disturbance that was used in a channel flow [14]. The initial localized disturbances in a form of longitudinal counter vortex pairs were defined by a stream function of $\psi = aX'Y'z'^3 \exp\left(-X'^2Y'^2z'^2\right)$, where and $X' = (x - x_c)\cos\theta_d - (y - y_c)\sin\theta_d$, and $Y' = (x - x_c)\sin\theta_d + (y - y_c)\cos\theta_d$. Here, θ_d is the inclination angle of the longitudinal vortices against the chordwise (x) direction, while y and z are the spanwise and wall-normal directions, respectively. In FSC boundary layer, the angle is defined as $\theta_d = \tan^{-1}(W_{\mathrm{FSC}}(x_c)/U_{\mathrm{FSC}}(x_c))$, where (x_c, y_c) is the center position of the initial disturbance $(x_c, y_c) = (6.285\delta_0^*, 100.56\delta_0^*)$. The detailed computational methods of direct numerical simulation were the same as in our previous study [15]. The computational domains size is of $(L_x, L_y, L_z)/\delta_0^* = (402.24, 201.12, 27)$ and the number of grids is $(N_x, N_y, N_z) = (2048, 1024, 160)$.

3 Results and discussion

We compared the developments of a turbulent spot between the FSC boundary layer and the Blasius boundary layer to discuss the peculiarities and their causes of the development process in the FSC boundary layer. Figures 1(a) and 1(b) show the spreading angle of the turbulent spot under each condition and the friction coefficient distribution used to calculate the spreading angle, respectively. As shown in Figure 1(a), the spreading angle in the FSC boundary layer is larger than that in the Blasius boundary layer for all initial disturbance amplitudes, a, in the present study. In two-dimensional boundary layers, Gostelow et al. [16] reported that the spreading angle of a turbulent spot in the accelerating gradient boundary layer is smaller than in the decelerating gradient boundary layer. However, results in the FSC boundary layer with an acceleration gradient indicate a larger spreading angle. These suggest that the effects of crossflow instability play a more dominant role in the spreading mechanisms than the effects of the velocity gradient. In the Blasius boundary layer, the spreading angles are similar regardless of the initial disturbance amplitude. On the other hand, in the FSC boundary layer, a dependence on the initial disturbance amplitude appears for $a < 8$. In the following, we compare the results for $a = 3.0$ in the Blasius boundary layer with those in the FSC boundary layer. In the FSC boundary layer, we mainly use the results for $a = 3.0$ and $a = 5.0$ to discuss the factors that led to the dependence of the spreading angle.

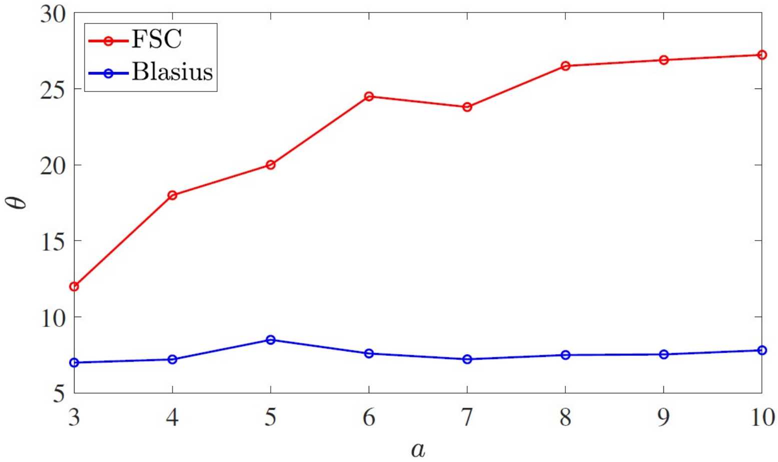

(a)

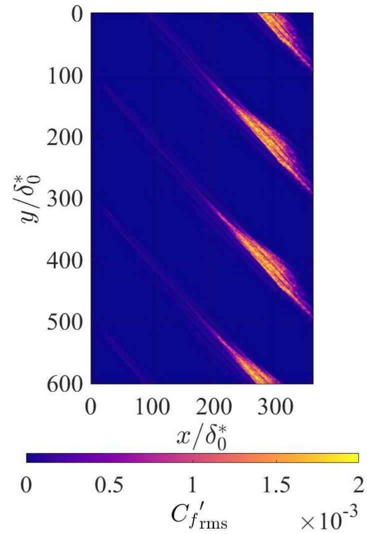

(b)

Figure 1: (a) Spreading angle θ dependency on the boundary layers. (b) RMS value of friction coefficient fluctuation $C_f' = C_f - C_{f,\mathrm{laminar}}$ for $a = 3.0$ in the FSC boundary layer.

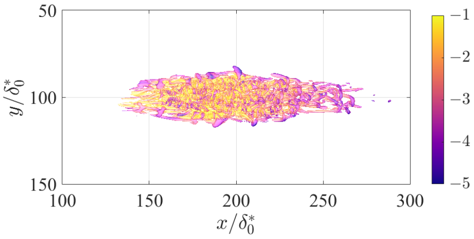

(a) Top view

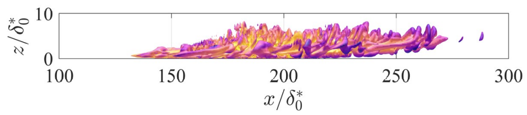

(b) Side view

Figure 2: Instantaneous flow fields for $a = 3.0$ in the Blasius boundary layer. Isosurface is vortex structures ($Q = 0.0005$) and colored by the kinetic eneryg ($\log(k)$).

We used the results for turbulent spots in the Blasius boundary layer to indicate the typical characteristics of the spreading process of turbulent spots. We show vortex structures of turbulent spots by the second invariant of the velocity gradient tensor (Q-value) in Figure 2. The isosurfaces are colored by the kinetic energy (log(k)) of the fluctuations. The kinetic energy is defined as $k = 0.5(u'^2 + v'^2 + w'^2)$, where the velocity fluctuation is $u'/U_0 = (u - u|_{\mathrm{laminar}})/U_0$ as the difference from the base flow. In the Blasius boundary layer, the turbulent spot becomes a Λ-shape, and we can observe hairpin vortices in the middle of turbulent spots with high kinetic energy. In Figure 2(b), we can observe that the vortex structure moves away from the wall in the downstream region of the turbulent spot. This structure is called an overhang and appears as the vortex structure generated far from the wall. These vortices move away from the body of the turbulent spot. On the upstream side of the turbulent spots, the visualized vortex structures appear in the near-wall region compared to the middle of the turbulent spots. The structure of the turbulent spots seen in Figure 2 is similar to that reported in many previous studies [17]. Zhao et al. [4] reported that the turbulent spots spread in the spanwise direction by secondary hairpin vortex generation from the primary hairpin vortex legs. Such a mechanism was independent of the initial disturbance amplitude.

Turbulent spots in the FSC boundary layer have different development mechanisms from those in the Blasius boundary layer. We show vortex structures for $a = 3.0$ and 5.0 in Figure 3 to discuss these mechanisms. In addition to the vortex structure visualized by Q-isosurface, Figure 3 shows the freestream direction at the outer edge of the boundary layer (blue line) and near the wall (red line). One of the differences from the Blasius boundary layer is the shedding vortices from the x-wise upstream side of the turbulence spot. This vortex shedding is independent of the initial disturbance amplitude, and the

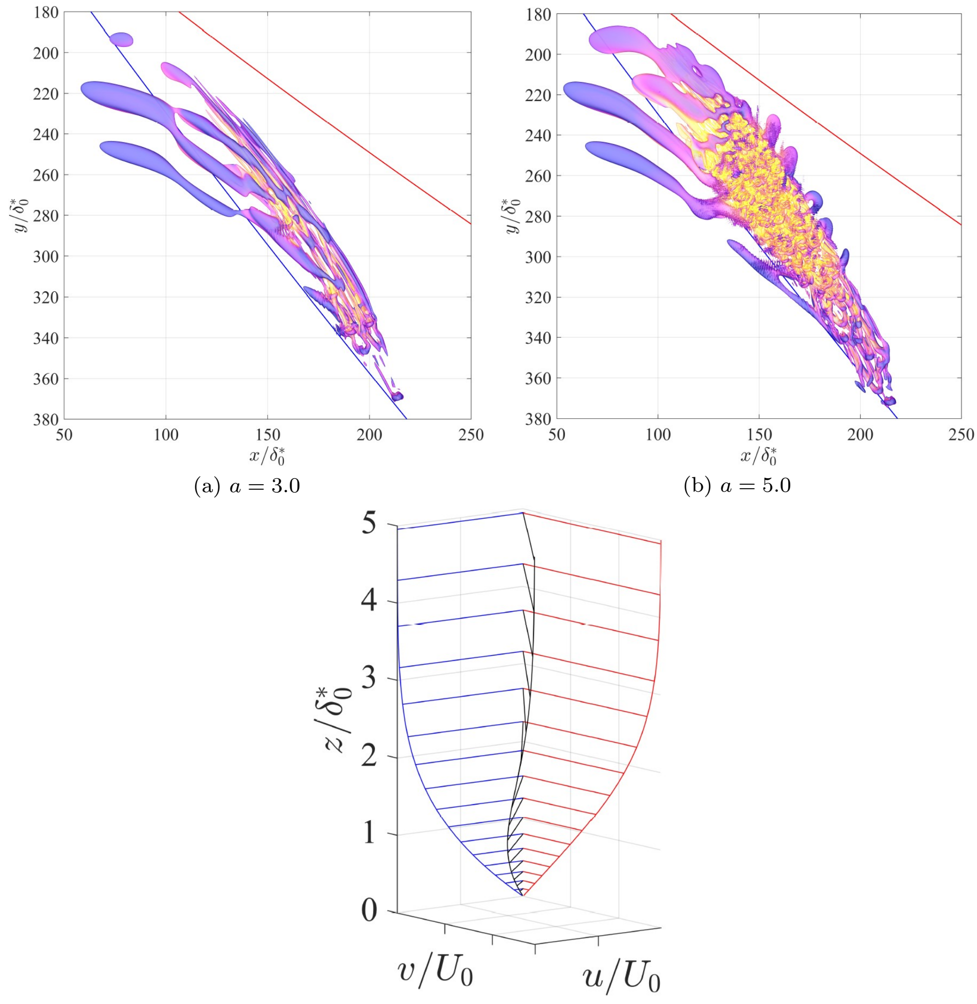

(a) $a = 3.0$

(b) $a = 5.0$

(c)

Figure 3: (a, b) Instantaneous flow fields for $a = 3.0$ and 5.0 in the FSC boundary layer. Isosurface is vortex structures ($Q = 0.0001$) colored by k. The color scale is same as figure 2. (c) Base flow profile at inlet.

vortex structures advect with the same vortex spacing in both cases. This phenomenon is consistent with the characteristics of the traveling crossflow vortex in the FSC boundary layer [18]. A previous study also shows that traveling crossflow vortices are more unstable than stationary vortices [13]. Experimental studies have also shown that traveling crossflow vortices generate from localized turbulent regions [3, 5]. Therefore, typical oblique waves around turbulent spots may have grown into traveling crossflow vortices in the FSC boundary layer. The shedding of traveling crossflow vortex is one of the causes of the turbulent spot spreading. Together with the spreading process caused by the hairpin vortices, this phenomenon supports the results of the comparison of the spreading angles for each boundary layer in Figure 1.

The growth process has other notable characteristics. While the turbulence spot in the Blasius boundary layer (Figure 2) is approximately symmetrical in the streamwise direction, the turbulence spot in the FSC boundary layer (Figure 3) is curved upstream in the spanwise direction. The twisted three-dimensional boundary layer shown in Figure 3(c) causes this phenomenon. Vortex structures downstream of the turbulent spot where the hangover occurs, i.e., far from the wall, advect downstream along the blue line in Figure 3. On the other hand, near-wall structures of turbulent spots tend to move away from the streamlines outside the boundary layer and closer to the streamlines near the wall. We conclude that the spatial spreading of the turbulent spot in the three-dimensional boundary layer is greater than in the Blasius boundary layer because the streamwise direction depends on the wall-normal height. The spanwise spreading caused by the boundary layer profile depends on the initial disturbance amplitude, with $a = 5.0$ forming a Λ-shape in the middle of the turbulence spot. In contrast, for $a = 3.0$, the traveling crossflow vortex dominates the vortex structure, and the high kinetic energy region formed by

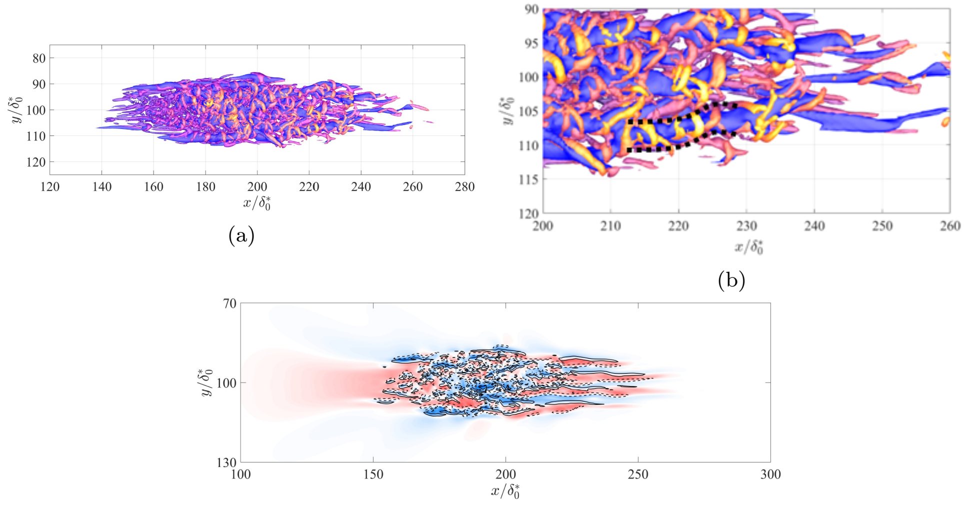

(a) (b) (c)

Figure 4: (a, b) Instantaneous flow fields for $a = 3.0$ in the Blasius boundary layer. Isosurfaces are vortex structures ($Q = 0.0005$) and low velocity region $u'/U_0 = -0.1$ (blue). Vortex structures are colored by wall-normal height $z/\delta_0^* = 0 - 8.0$. (c) Colormap indicates fluctuation velocity distribution ($u'/U_0 = \pm 0.8$) and contour lines indicate spanwise velocity gradient $\partial u/\partial y = 0.15$ (solid line) and $\partial u/\partial y = -0.15$ (dash line) at $z/\delta_0^* \approx 2.0$.

the hairpin vortex group is limited to the near-wall region. Note, because of the shedding of the traveling crossflow vortex and the twisted velocity profile, the spreading angle is higher than the angle for the Blasius boundary layer (see Figure 1).

We discuss the mechanism of spatial spreading and the differences between the boundary layers. The spanwise spreading of the hairpin vortex leads to the induction of Kelvin–Helmholtz instability owing to high shear in the spanwise direction, as the hairpin head causes wavy distortions to the streak structure in the boundary layer [19]. This results in distorted hairpin vortices in the streamwise direction and the spreading of turbulent spots. To confirm this mechanism in the Blasius boundary layer, we show a three-dimensional visualization and fluctuation distribution in the x–y plane at $z/\delta_0^* \approx 2.0$ in Figure 4. Figure 4(a, b) show isosurfaces for the vortex structure by Q-value and low-velocity region by $u'/U_0 = (u - u|_{\text{laminar}})/U_0 = -0.1$. The rotation of the hairpin vortex lifts the low-speed fluid away from the wall (ejection) and supplies the high-speed fluid to the near wall (sweep) [20, 21]. Therefore, the fluid surrounded by hairpin vortices forms a low-speed streak, as shown in Figure 4. The enlarged view in Figure 4(b) captures in detail the distortion of the streak structure that leads to the spreading of the turbulent spot. Hairpin vortex arrays occur along these low-speed streaks that are wavy and distorted to the streamwise direction. These localized distortions contribute to turbulent spot spreading with the formation of new wavy streaks as time progresses. Figure 4(c) shows the wavy distortion of the streak structure and the resulting formation of high-shear regions. The analysis of vortex structures and velocity distribution reveals the same trend as in previous studies [19]: the formation of high shear and the resulting spreading of the disturbed region.

Previous studies [2, 22] reported that hairpin vortices occur from a high cylindrical roughness, and the turbulent region spreads the whole spanwise region in the three-dimensional boundary layer. The rotation of the hairpin vortex, the sweep, and ejection events are similar to those of wall turbulence as same as the Blasius boundary layer. Figure 5(a) shows hairpin vortices and the fluid dynamics around the hairpin vortices. As in the visualization of turbulent spots in the Blasius boundary layer, a low-speed streak structure occurs between the hairpin vortices. The vortex structure colored by wall-normal height also shows overhangs in the spanwise direction, similar to downstream of the streamwise direction. This spanwise overhang is due to a spanwise component of the FSC boundary layer. We identified that the asymmetry structure in the wall-normal direction is one of the characteristics of the spreading mechanism in a crossflow instability-dominated flow field. A previous study on the spreading turbulent regions by super-critical roughness height ($Re_{kk} > 2800$) also reported an unbalanced distribution [3]. This characteristic is consistent with the tendency for the spreading characteristic of a turbulent spot. A large low-speed streak is visible upstream of the turbulent spot in Figure 5(a). This streak is due to the low-speed fluid lifted from near the wall by the traveling crossflow vortex. However, all low-speed

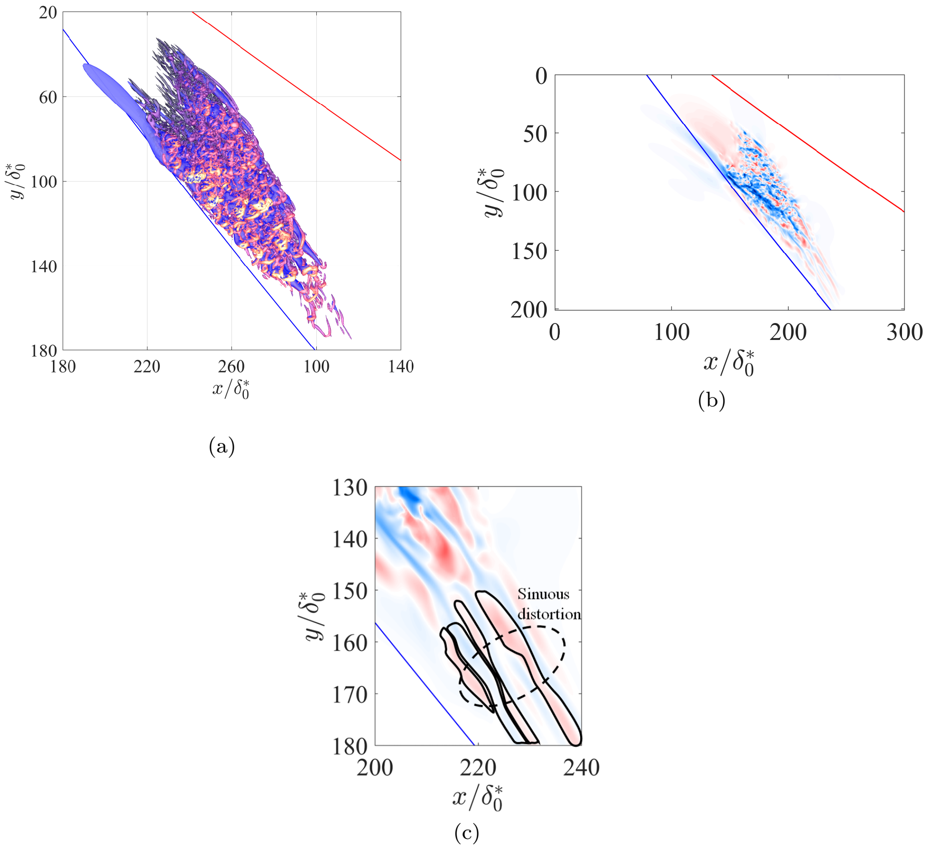

Figure 5: (a) Instantaneous flow fields for $a = 5.0$ in the FSC boundary layer. Isosurfaces are vortex structures ($Q = 0.001$) and low velocity region $u'/U_0 = -0.1$ (blue). Vortex structures are colored by wall-normal height $z/\delta_0^* = 0 - 8.0$. (b, c) Colormap indicates fluctuation velocity distribution ($u'/U_0 = -0.8$ (blue) to 0.8 (red)) at $z/\delta_0^* \approx 2.5$.

streaks formed by the multiple vortex structures in Figure 3(b) are not directly visualized in Figure 5(a).

We investigate the spreading mechanism of the turbulent spot structure by u' distribution in the x–y plane at $z/\delta_0^* \approx 2.5$ in Figure 5(b). In this fluctuation distribution, the base flow is in the same direction while the streak structure is curved: the downstream streak closes to the direction of the streamlines outside the boundary layer, and the upstream structure closes to the direction of the streamlines near the wall. At the downstream end of the streak structure, the hangover brings the legs of the hairpin vortex from outside the boundary layer. Owing to this phenomenon, the streak direction is along the outside streamwise direction. Upstream of the turbulent spots, the legs tend to extend in the streamwise direction at visualized height and in the streamwise direction near the wall, resulting in curved streaks.

We focus on the wavy distortion of the streak caused by the twisted boundary layer, as shown in Figure 5(c). The sinuous distortion caused by the boundary layer can contribute to the turbulent region spreading, as in previous studies [19]. Figure 5(b) shows that this phenomenon occurs not only at the point shown in Figure 5(c) but also in several stages throughout the turbulent spot development. In other words, we conclude that because of the twisted boundary layer, the turbulence region caused by the hairpin vortices is more likely to be spread out compared to a two-dimensional boundary layer. In addition to the fact that turbulent transitions are promoted in swept flat plates and swept wings, compared to Tollmien–Schlichting-wave-dominated flow fields, due to the crossflow instability, this study has clarified that crossflow instability can also enhance the turbulent region spreading.

4 Conclusion

We investigated the development process of turbulent spots in the FSC boundary layer dominated by crossflow instability using direct numerical simulation. By comparing with the development process of turbulent spots in the Blasius boundary layer, we have clarified the characteristics of the spreading of turbulent regions in the FSC boundary layer. The process of turbulent spot spreading goes through the generation of hairpin vortices, sinuous distortion of the streak structure caused by the hairpin vortices, Kelvin–Helmholtz instability caused by the sinuous distortion, and new hairpin vortices induced by the instability. During the development process, the FSC boundary layer and the Blasius boundary layer show significant differences in the spreading angle, with the FSC boundary layer having a greater angle. This is caused by the characteristics of the FSC boundary layer. First, in the FSC boundary layer, traveling crossflow vortices generate from turbulent spots. These vortex structures advect in the spanwise direction and thus contribute to the spreading of the turbulent region. However, we cannot capture the growth of traveling vortices into turbulence in this calculation region, so its contribution to the turbulent region spreading is unclear. Secondly, owing to the twisted boundary layer, the turbulent region spreads in different directions inside and outside the boundary layer. This velocity profile causes the turbulent spots to spread asymmetrically in the streamwise direction, resulting in a curved Λ-shape structure. Finally, the twisted boundary layer also affects the process of turbulent spot spreading. We found that the legs of the hairpin vortex curve in the direction of the base flow as they penetrate the boundary layer. These curved legs directly lead to a wavy distortion of the streak structure. This wavy structure promotes the generation of new hairpin vortices, as reported by previous studies on the spreading of turbulent regions in 2D boundary layers. We found that turbulent spot spreading in the FSC boundary layer with a twisted boundary layer is superior to that in the Blasius boundary layer because of the reasons mentioned above.

The spreading process of the turbulent region revealed in this study can also occur in swept wings, which is dominated by the crosslow instability. The knowledge obtained from this study will contribute to the prediction of the local turbulence spreading over the whole surface of the wing. It will increase accuracy in predicting a transition point from an engineering perspective. Future work is still remaining to clarify the shedding mechanism of the traveling crossflow vortex and to formulate the relationship between the swept angle, i.e., contribution of crossflow instability, and the spreading of the turbulent region.

Acknowledgment

The author K.N. was supported by JST SPRING, Grant No. JPMJSP2151. We used the supercomputer resources of Osaka Univ. Cybermedia Center and Tohoku Univ. Cyberscience Center.

References

[1] W. S. Saric, H. L. Reed, and E. B. White. Stability and transition of three-dimensional boundary layers. *Annu. Rev. Fluid Mech.*, 35(1):413–440, 2003.

[2] M. Brynjell-Rahkola, N. Shahriari, P. Schlatter, A. Hanifi, and D. S. Henningson. Stability and sensitivity of a cross-flow-dominated Falkner–Skan–Cooke boundary layer with discrete surface roughness. *J. Fluid Mech.*, 826:830–850, 2017.

[3] T. Ishida, K. Ohira, R. Hosoi, N. Tokugawa, and T. Tsukahara. Numerical and experimental analysis of three-dimensional boundary-layer transition induced by isolated cylindrical roughness elements. *Int. J. Aeronaut. Space Sci.*, 23(4):649–659, 2022.

[4] J. Yoshikawa, Y. Nishio, S. Izawa, and Y. Fukunishi. Key structure in laminar-turbulent transition of boundary layer with streaky structures. *Theor. Appl. Mech.*, 9(1):32–35, 2019.

[5] A. Nishizawa, S. Takagi, and N. Tokugawa. Transition of wave packets originating from localized strong disturbances in laminar boundary-layer of rotating-disk flow. In *TSFP2*, pages 75–80, 2001.

[6] M. Matsubara and P. H. Alfredsson. Disturbance growth in boundary layers subjected to free-stream turbulence. *J. Fluid Mech.*, 430:149–168, 2001.

[7] T. A. Zaki. From streaks to spots and on to turbulence: Exploring the dynamics of boundary layer transition. *Flow Turbul. Combust.*, 91:451–473, 2013.

[8] P. Andersson, Brandt L., Bottaro A., and Henningson D. S. On the breakdown of boundary layer streaks. *J. Fluid Mech.*, 428:29–60, 2001.

[9] J.-Ch Loiseau, J.-Ch Robinet, S. Cherubini, and E. Leriche. Investigation of the roughness-induced transition: global stability analyses and direct numerical simulations. *J. Fluid Mech.*, 760:175–211, 2014.

[10] M. A. Bucci, D. K. Puckert, C. Andriano, J.-Ch Loiseau, S. Cherubini, J.-Ch Robinet, and U. Rist.

Roughness-induced transition by quasi-resonance of a varicose global mode. *J. Fluid Mech.*, 836:167–191, 2018.

[11] A. Weingärtner, S. B. Mamidala, and J.H.M. Fransson. Instabilities in the wake of an isolated cylindrical roughness element. *J. Fluid Mech.*, 960:A8, 2023.

[12] J. C. Cooke. The boundary layer of a class of infinite yawed cylinders. *Math. Proc. Camb. Philos. Soc.*, 46(4):645–648, 1950.

[13] M. Högberg and D. Henningson. Secondary instability of cross-flow vortices in Falkner–Skan–Cooke boundary layers. *J. Fluid Mech.*, 368:339–357, 1998.

[14] D. S. Henningson and J. Kim. On turbulent spots in plane Poiseuille flow. *J. Fluid Mech.*, 228:183–205, 1991.

[15] K. Nakagawa, T. Ishida, and T. Tsukahara. Effects of freestream turbulence on the secondary instability of the roughness-induced crossflow vortex in swept flat plate boundary layers. *Int J Heat Fluid Flow*, 102:109161, 2023.

[16] J. P. Gostelow, N. Melwani, and G. J. Walker. Effects of streamwise pressure gradient on turbulent spot development. *J. Turbomach.*, 118:737–743, 1996.

[17] X. Wu. New insights into turbulent spots. *Annu. Rev. Fluid Mech.*, 55:45–75, 2023.

[18] P. Wassermann and M. Kloker. Transition mechanisms induced by travelling crossflow vortices in a three-dimensional boundary layer. *J. Fluid Mech.*, 483:67–89, 2003.

[19] Y. Zhao, S. Xiong, Y. Yang, and S. Chen. Sinuous distortion of vortex surfaces in the lateral growth of turbulent spots. *Phys. Rev. Fluids*, 3:074701, Jul 2018.

[20] S. K. Robinson. Coherent motions in the turbulent boundary layer. *Annu. Rev. Fluid Mech.*, 23(1):601–639, 1991.

[21] R. J. Adrian. Hairpin vortex organization in wall turbulencea). *Phys. Fluids*, 19(4):041301, 2007.

[22] K. Nakagawa, T. Tsukahara, and T. Ishida. DNS study on turbulent transition induced by an interaction between freestream turbulence and cylindrical roughness in swept flat-plate boundary layer. *Aerospace*, 10(2), 2023.